International Journal of Technology and Applied Science (IJTAS)
E-ISSN: 2230-9004 ● Website: www.ijtas.com ● Email: editor@ijtas.com

Carbon Nanotubes in Nanoscience: Structural Features, Electronic Properties, and Emerging Applications

Dr. Jyoti Mishra

Assistant Professor, Department of Physics, D.B.S. College, Govind Nagar, Kanpur, U.P.

Abstract

A carbon nanotube is a sheet of graphene rolled into a closed cylinder, and the way the sheet is rolled decides almost everything about it. Two integers, the chiral indices (n, m), fix the diameter, the twist of the hexagons around the axis, and whether electrons see a metal or a semiconductor. This review follows that idea from the lattice to the device. We work through the zone-folding picture, which predicts that about one tube in three is metallic and that the gap of the rest falls as the inverse of diameter, and we compute the gap for every tube between 0.6 and 2.0 nm using constants taken from the literature. Scanning tunnelling microscopy, resonant Raman scattering and optical absorption have tested these predictions closely, and we set the model against what those measurements found. The small curvature gaps that make many "metallic" tubes slightly semiconducting get a short treatment of their own. The review then turns to the practical side: growth by arc discharge, laser vaporization and chemical vapour deposition, and sorting by density, gel affinity, aqueous phases and polymer wrapping. Applications covered include transistors and full processors, interconnects, transparent films, chemical and biological sensors, battery electrodes, composites and biomedical devices. The toxicity of long, rigid tubes is treated as a design constraint rather than a footnote.

Keywords: carbon nanotubes; chirality; band structure; ballistic transport; Raman spectroscopy; nanoelectronics

1. Introduction

In 1991 Iijima reported needle-like deposits on the negative electrode of a carbon arc and showed, by electron microscopy, that each needle was made of coaxial graphitic tubes, from 2 up to about 50 of them, a few to a few tens of nanometres across [1]. The hexagons on each tube wound helically about the axis. Within two years, tubes with walls only one atom thick had been grown as well, with diameters close to a nanometre. Most of the physics below concerns that single-walled form.

Theory had moved quickly, and two groups reached the same striking conclusion within months. Saito and co-workers found that roughly one third of all possible tubes should be one-dimensional metals and the other two thirds' semiconductors [2]. Hamada, Sawada and Oshiyama predicted that conduction could range from metallic to semiconducting with narrow or moderate gaps, depending only on diameter and helical arrangement [3]. Their argument needed little more than the band structure of a single graphite sheet and a boundary condition around the tube [3], which is why it could be made so fast, before anyone had a single tube to measure.

So the same element, bonded the same way, could be either a wire or a semiconductor. Few predictions in materials physics have been tested as directly. In January 1998 Wildöer and co-workers published atomically resolved scanning tunnelling microscope images of individual single-walled tubes next to their tunnelling spectra, and saw the expected link between wrapping geometry and electronic character [4]. A few months later a single semiconducting nanotube between two metal contacts was switched on and off by a gate voltage at room temperature [5].

The road from that transistor to a working processor took two decades, and it ran through problems the early papers barely mentioned: making one kind of tube, contacting it without a large barrier, and living with the metallic tubes that always slip through. A 16-bit microprocessor with more than 14,000 nanotube transistors was reported in 2019 [6], and a tensor processing unit built from 3,000 of them followed in 2024 [7].

This is a literature-based account for readers who know some solid-state physics. It reports no new experiments; the band-gap graph is a calculation from the equations in the text.

2. Structure and Classification

Start with graphene. Its honeycomb lattice has two atoms per unit cell, a carbon to carbon bond length a_CC = 0.142 nm, and primitive vectors a1 and a2 of length a = √3 a_CC = 0.246 nm at 60 degrees to each other. Choose any lattice vector

$$Ch = n\,a1 + m\,a2$$

and roll the sheet so that the two ends of Ch meet, giving a tube of circumference |Ch|. The pair of integers, with $n \geq m \geq 0$, is the chiral index.

The diameter follows at once from the length of Ch:

$$d = (a/\pi)\,\sqrt{(n^2 + nm + m^2)}$$

For a (10, 10) tube this gives 1.36 nm, and for a (13, 0) tube 1.02 nm. A second number, the chiral angle θ, measures how far Ch is tilted from the zigzag direction, with $\tan\theta = \sqrt{3}\,m / (2n + m)$. It runs from 0 to 30 degrees.

When m = 0 the tube is called zigzag, because a cut across the axis traces a zigzag line of bonds. When n = m it is called armchair, after the shape of the same cut. Everything in between is chiral and, like a screw, differs from its mirror image. The names are purely geometric. (The electrons, it turns out, care about n and m in a way these names do not capture.)

Real tubes are rarely this simple. Iijima's first samples were multi-walled: shells nested one inside another, each with its own chiral index [1]. The gap between neighbouring shells is close to the interlayer spacing of graphite. Figure 1 shows a model of such a tube with three armchair shells.

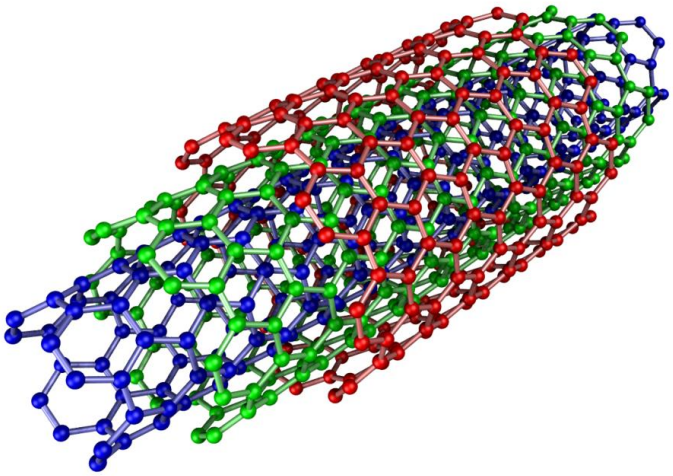


Figure 1. Ball-and-stick model of a multi-walled armchair carbon nanotube with three coaxial shells, each drawn in a different colour. Image: Eric Wieser, Wikimedia Commons, CC BY-SA 3.0, https://commons.wikimedia.org/wiki/File:Multi-walled_Carbon_Nanotube.png

Each shell in the model is a complete tube, and real shells need not share a chiral angle, so a multi-walled tube is several electronic systems held together by weak interlayer forces. Measurements often probe only the outer one. The tensile tests of Yu and co-workers are a good example: the tubes broke in the outermost layer, in what the authors called sword-in-sheath failure [8].

Single-walled tubes, by contrast, usually come in a narrow diameter range set by the growth chemistry, and they like to pack side by side into bundles, often called ropes. The ropes matter. Tubes in a bundle touch along their whole length and feel each other, which shifts their electronic levels a little; this is one reason spectroscopists go to some trouble to isolate single tubes before measuring them.

Defects complete the picture. Real tubes have vacancies, pentagon and heptagon pairs, adsorbed molecules and changes of chiral index along their length. Such flaws scatter electrons and show up as the disorder-induced D band in the Raman spectrum. In circuits they appear statistically, as a spread in device behaviour that designers must absorb [6].

3. Electronic Properties

3.1 Zone folding

Graphene's π bands touch at the corners of its Brillouin zone, the K points, where the dispersion is linear. Rolling the sheet adds one rule: the wavefunction must return to itself after a trip around Ch. Wavevectors around the circumference are then quantized, and the two-dimensional bands are cut into a set of one-dimensional subbands along allowed lines.

Whether the tube is a metal depends on one question. Does any allowed line pass through a K point? If it does, two linear bands cross at the Fermi level and the tube conducts like a one-dimensional metal. If not, the nearest line misses K by a finite distance and a gap opens. Working through the geometry gives a compact rule: the tube is metallic when (n − m) is divisible by 3, and semiconducting otherwise [2], [3].

Every armchair tube is therefore metallic, and a zigzag tube is metallic only when n is a multiple of 3. We can check the one-third fraction directly: of the 195 distinct (n, m) pairs with diameters between 0.6 and 2.0 nm, 68 satisfy (n − m) mod 3 = 0, which is 35 percent.

For the semiconducting two thirds, the distance from the nearest allowed line to K scales as 1/d, and near K the bands are linear with a slope set by the nearest-neighbour hopping energy γ0. The gap therefore takes a simple form,

$$E_g = 2\, a_{CC}\, \gamma_0 / d$$

which, to first order, ignores chiral angle. Fitted values of γ0 lie near 2.7 to 2.9 eV; we use 2.9 eV, the value Jorio and co-workers adopted when they assigned the chiral indices of individual tubes from Raman data [9]. With a_CC = 0.142 nm the product 2 a_CC γ0 comes to 0.82 eV nm. A 1.0 nm tube then has a gap near 0.82 eV, a 1.4 nm tube near 0.59 eV, and a 2.0 nm tube near 0.41 eV. Choosing 2.7 eV instead would lower each of these by 7 percent.

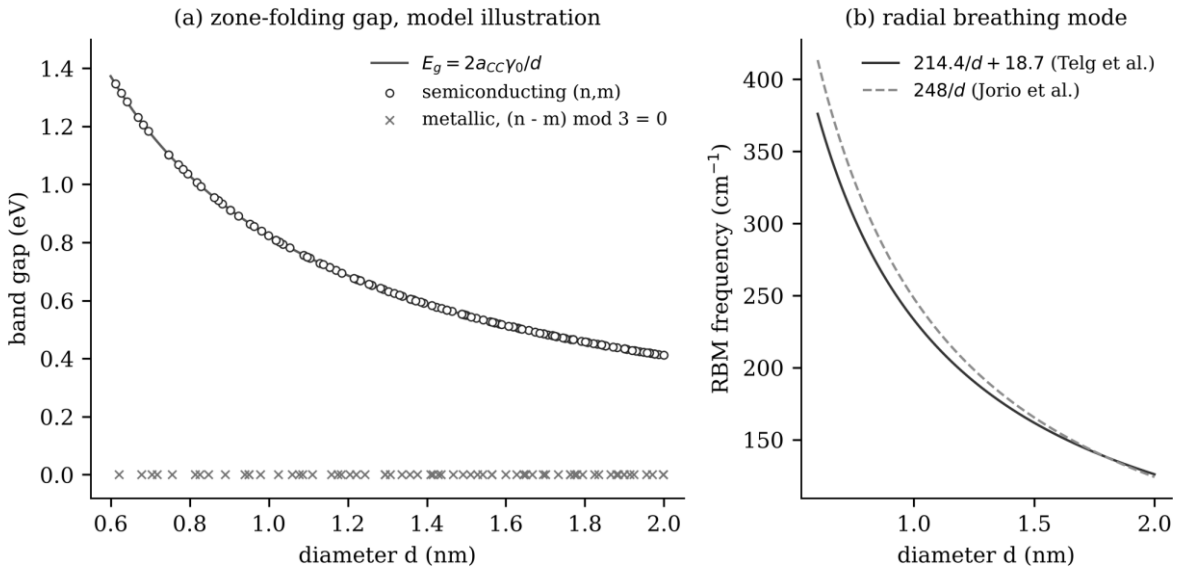


Figure 2. Model illustration computed from the equations in this paper, not measured data. (a) Band gap against diameter for all 195 chiral indices with 0.6 nm ≤ d ≤ 2.0 nm. Open circles are semiconducting tubes from E_g = 2 a_CC γ0 / d with a_CC = 0.142 nm and γ0 = 2.9 eV (the value used by Jorio et al. [9]); the line is the same 1/d law; crosses are tubes with (n − m) mod 3 = 0, placed at zero gap, so curvature gaps are ignored. Diameters use d = (a/π)√(n² + nm + m²) with a = 0.246 nm. (b) Radial breathing mode frequency against diameter from the empirical relations ω = 214.4/d + 18.7 cm⁻¹ of Telg et al. [10] and ω = 248/d cm⁻¹ of Jorio et al. [9].

Panel (a) of Figure 2 shows how sharp the prediction is. Semiconducting tubes lie on one curve and metallic ones sit in a row at zero, interleaved at nearly every diameter. Shift one index, from (13, 0) to (12, 0), and a tube jumps rows. That is why growth control and sorting matter so much. Panel (b) previews a link used later: the breathing mode tracks the same diameter.

3.2 What the simple picture misses

But the wall is curved, and curvature mixes σ and π orbitals and shifts the K point slightly. For armchair tubes symmetry protects the band crossing. For other tubes with (n − m) divisible by 3 it does not, and a small secondary gap opens. Simple estimates make this gap scale as 1/d², against 1/d for the main gap, so it shrinks fast with size; for tubes near a nanometre it is a small fraction of the semiconducting gap at the

same diameter. At room temperature such tubes still behave much like metals. At low temperature, or when neighbouring tubes in a bundle break the symmetry, the difference can show. So "metallic" in the zone-folding sense really means "gapless or nearly so". Table 1 sets the main classes side by side with these refinements included.

Table 1. Main classes of carbon nanotube compared. Diameters for the example indices come from $d = (a/\pi)\sqrt{(n^2 + nm + m^2)}$ with $a = 0.246$ nm and gaps from $E_g = 2\, a_{CC}\, \gamma_0 / d$ with $\gamma_0 = 2.9$ eV; other entries are from the cited sources.

Class	Example (n, m)	Diameter	Electronic character	Key property	Representative use
Armchair	(10, 10)	1.36 nm (formula)	Metallic; band crossing protected by symmetry (zone folding) [2]	Ballistic limit $4e^2/h$ per tube [11]	Wiring, in principle
Zigzag, n divisible by 3	(12, 0)	0.94 nm (formula)	Metallic in zone folding; small curvature gap expected	Sensitive to curvature and bundling	Test case for band theory
Zigzag, other n	(13, 0)	1.02 nm (formula)	Semiconducting, E_g about 0.81 eV (formula)	Gap set by diameter [2], [3]	Transistor channel [5]
Chiral, metallic	(13, 10)	1.56 nm (formula)	Metallic, since $13 - 10$ is divisible by 3	Assigned from one RBM line at 156 cm^{-1} [9]	Test case for Raman (n, m) assignment [9]
Chiral, semiconducting	(8, 6)	0.95 nm (formula)	Semiconducting, E_g about 0.86 eV (formula)	Gap in the near infrared (formula)	Transistor and sensor channels [7], [12]
Multi-walled	2 to about 50 shells [1]	A few to a few tens of nm [1]	Conductance quantum $2e^2/h$ measured on arc-grown tubes [13]	Outer-shell strength 11 to 63 GPa [8]; stable current density above 10^7 A cm^{-2} [13]	High-current wiring and composites [13], [8]

3.3 Van Hove singularities and the STM tests

A one-dimensional subband has a density of states that diverges as $1/\sqrt{E}$ at its edge. These spikes, the van Hove singularities, sit in pairs about the Fermi level; in a semiconducting tube the first pair is separated by E_g.

The 1998 STM work tested all of this on single tubes. Wildöer and co-workers took atomically resolved images and tunnelling spectra on the same tubes and found metallic and semiconducting tubes, gaps consistent with theory, and sharp peaks at the onsets of the one-dimensional bands [4]. The method is worth spelling out, because it is the cleanest test the field has. The tip first maps the atoms, which gives the wrapping angle and the diameter; then, held over the same tube, it records how the tunnelling current

changes with bias, which traces the density of states. Structure and electronic character come from one tube in one experiment. Figure 3 shows an image of this kind.

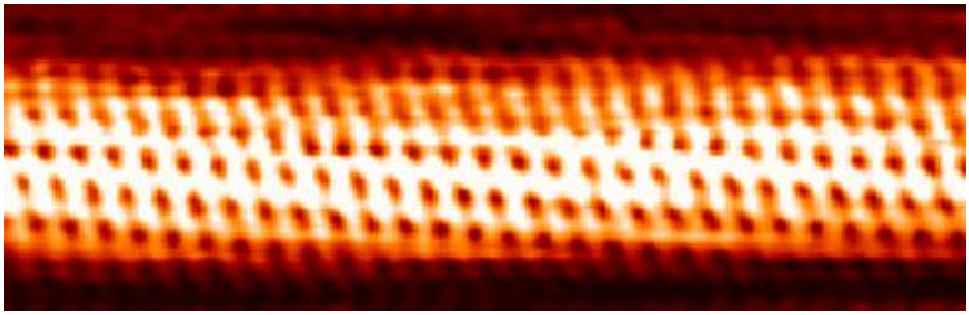


Figure 3. Atomically resolved scanning tunnelling microscope image of a single chiral carbon nanotube; the rows of bright features wind around the tube axis at an angle set by the chiral index. Image: Taner Yildirim, National Institute of Standards and Technology (NIST), via Wikimedia Commons, public domain (US government work), https://commons.wikimedia.org/wiki/File:Chiraltube.png

The tilted rows are the point. On a zigzag or armchair tube they would run along or across the axis; here they run at an angle, so the image gives θ directly. Add a diameter and you have (n, m), and with it a definite electronic prediction that the tip can then check on the same tube.

3.4 Optical transitions and the Kataura plot

Light couples most strongly to transitions between mirror-image singularities, E11, E22 and so on. Plotting these energies for every tube in a diameter range against diameter gives the chart known as the Kataura plot, after the first author of the paper that popularized it. Each transition forms a band of points that roughly follows 1/d but scatters with chiral angle. It is the working map of the field. Telg and co-workers assigned about fifty tubes using a third-neighbour tight-binding Kataura plot together with Raman data [10].

3.5 Transport, contacts and barriers

A metallic tube has two subbands crossing the Fermi level, each with two spin states. In the Landauer picture each perfectly transmitting channel adds e^2/h, so one tube has a limit of $4e^2/h$, about 6.5 kΩ, whatever its length, provided electrons cross without scattering. Frank and co-workers dipped multi-walled tubes into liquid metal and found conductance quantized at one unit of $G0 = 2e^2/h$, which is $(12.9\ k\Omega)^{-1}$; the tubes, typically 15 nm wide and 4 μm long, carried current ballistically without heating and sustained current densities above 10^7 A cm^{-2} [13].

In a transistor the contact usually dominates. Where metal meets a semiconducting tube, the band alignment forms a Schottky barrier, and early nanotube transistors were limited by it. Javey and co-workers used palladium, which has a high work function and wets nanotubes well, and found that the barrier for holes almost disappeared [11]. Their devices reached room-temperature conductance close to $4e^2/h$, carried about 25 μA per tube, and showed Fabry-Perot interference at low temperature, the signature of phase-coherent electrons bouncing between two ends. At high bias the current saturated, set by backscattering from optical phonons.

Picture the contact as a narrow gate in a wall: electrons must tunnel through the barrier or be thermally kicked over it. Lower the step, as palladium does, and the gate opens. A ballistic channel is of little use behind a shut gate, which is why contact resistance became a headline figure.

4. Synthesis, Sorting and Characterization

4.1 Growth

Three routes have dominated. The first is arc discharge, where a current between graphite electrodes vaporizes carbon. Iijima's multi-walled tubes grew on the cathode this way [1], and adding a metal catalyst to the arc gives single-walled tubes instead. The second is laser vaporization, in which a pulsed laser evaporates a graphite target mixed with a little metal inside a hot furnace. It gives clean single-walled tubes with a fairly narrow spread of diameters, but in small amounts.

The third route, chemical vapour deposition, decomposes a carbon-bearing gas on catalyst particles. It runs at lower temperature than the other two and can grow tubes directly on a substrate, which is why it is the natural choice for chips. Its central problem has been chirality. A catalyst particle that is soft or mobile at growth temperature has no reason to favour one (n, m), so as-grown samples are mixtures, and metallic tubes turn up alongside semiconducting ones. Catalysts that keep a fixed crystal structure during growth can tip that balance. But growth of a single chirality, on demand and at scale, is still a goal rather than a routine process.

4.2 Sorting after growth

Most samples are mixtures, so separation after growth has carried much of the load. Four ideas dominate, and each exploits a small structural difference. Density-gradient ultracentrifugation wraps tubes in surfactants whose packing depends on diameter and electronic type, so tubes of different structure end up with slightly different buoyant densities and settle at different heights in a spinning gradient.

Gel chromatography uses the fact that tubes stick to a gel with a strength that depends on structure, so different species leave the column at different stages.

Aqueous two-phase extraction lets tubes distribute themselves between two immiscible water-based phases, and the balance can be tuned with surfactants until one species prefers one phase.

Polymer wrapping works in organic solvents: certain conjugated polymers coil around some tubes far more readily than others and carry them into solution, while the rest settle out.

For electronics, though, the number that counts is semiconducting purity, and it has to be extreme. The 2024 tensor processor used nanotubes with a stated semiconducting purity of 99.9999 percent [7]. A short estimate shows why. A transistor whose channel holds one metallic tube cannot be switched fully off, so at 99 percent purity a circuit with ten thousand tube channels would carry about a hundred such leaks. At 99.9999 percent the same circuit would expect a hundredth of one.

4.3 Raman scattering

If you could use only one tool on a nanotube sample, it would probably be a Raman spectrometer. The radial breathing mode, in which all atoms move in and out in phase, has a frequency inversely proportional to diameter,

$$\omega_RBM = A/d + B$$

where A and B depend somewhat on the environment. Jorio and co-workers, working on isolated tubes on a silicon substrate, used $\omega_RBM = 248/d$ with ω in cm^{-1} and d in nm, and showed that one RBM

frequency together with resonance theory is enough to assign (n, m) for a single tube [9]. Telg and co-workers, from about fifty tubes, found A = 214.4 cm^{-1} nm and B = 18.7 cm^{-1} [10]. Panel (b) of Figure 2 compares the two relations. They agree within a few percent above 1.5 nm and drift apart for small tubes, where a 0.6 nm tube would sit near 376 cm^{-1} on one curve and 413 cm^{-1} on the other.

The G band, from tangential stretching of the carbon bonds, sits near 1590 cm^{-1}. In a tube it splits in two, because curvature makes stretching along the axis differ from stretching around the circumference. The lower peak moves further down in thin tubes, and in metallic tubes it also broadens, so its shape hints at electronic type.

The D band needs a defect. It arises from a double-resonance process in which an electron scatters once off a phonon and once off a defect, so its height relative to the G band is a routine gauge of disorder. A weak D band means a clean lattice.

4.4 Optical and microscopic probes

Optical absorption of a dispersed sample shows peaks at the E11, E22 and metallic transitions, and reading them against the Kataura plot gives the mix of diameters in bulk. Microscopy gives the local view. Transmission electron microscopy counts shells and measures diameters; it was in electron micrographs that the helical arrangement of hexagons was first seen [1]. Scanning tunnelling microscopy resolves the lattice and the density of states on the same tube [4]. Neither scales to a wafer.

5. Emerging Applications

5.1 Transistors and logic

The band structure points to an almost ideal channel, one atom thick, with a gap chosen by diameter. Tans and co-workers built the first room-temperature device from one tube and two electrodes in 1998 [5]. By 2003 palladium contacts had made the on state nearly ballistic [11].

Circuits were harder. Designing around the imperfections inherent in nanotubes, Shulaker and co-workers in 2013 showed the first computer made entirely of nanotube transistors, running a simple multitasking operating system and 20 instructions from the commercial MIPS set [14]. Hills and co-workers scaled that approach into a 16-bit RISC-V microprocessor with more than 14,000 complementary transistors, designed and fabricated with industry-standard flows [6]. And a single tube per transistor is not enough. A practical device needs many parallel tubes in its channel, all aligned and evenly spaced across a whole wafer, so that current adds up and tube-to-tube differences average out.

How much current could such an array deliver? We can estimate it from the single-tube figure. Javey's palladium-contacted tubes carried about 25 µA each [11]. Suppose a channel holds 100 tubes per micrometre of width and each carries only a few microamperes under realistic bias. The total is then a few hundred microamperes to about a milliampere per micrometre. The estimate is crude, but it explains why contacts and density, not the tubes themselves, set the limit. The latest system-level result is a tensor processing unit of 3,000 transistors in a systolic array [7]. Running a five-layer convolutional network, it recognized handwritten digits with up to 88 percent accuracy at 295 µW. The authors estimated by simulation that an 8-bit version at a 180 nm node could reach 850 MHz and about one tera-operation per second per watt.

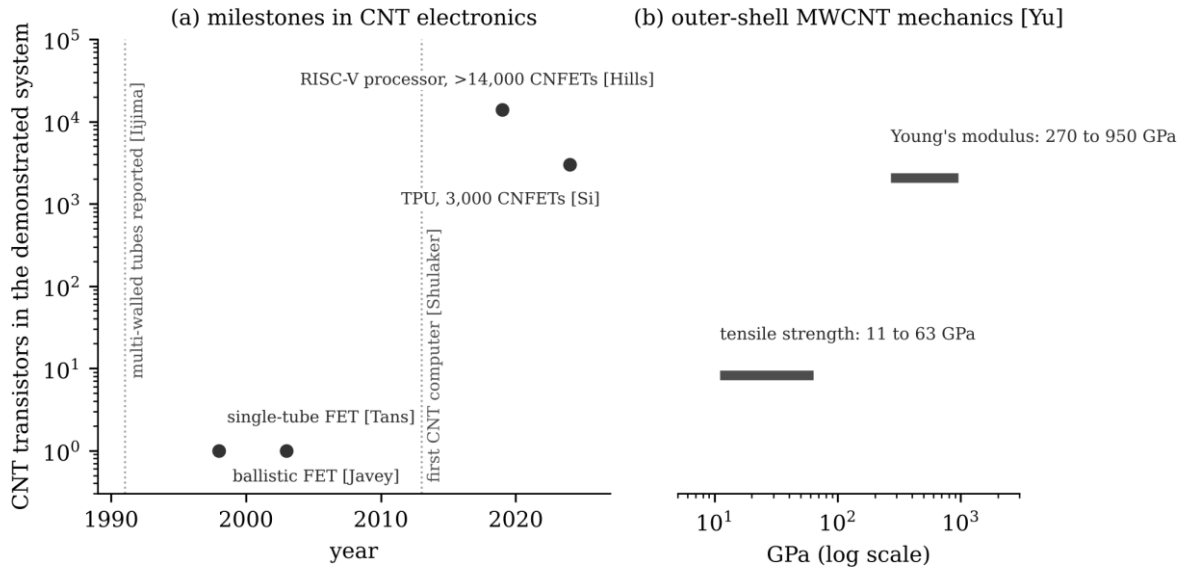


Figure 4. Reported figures from verified sources, plotted for comparison. (a) Number of carbon nanotube transistors in demonstrated systems against year of publication: a single-tube room-temperature transistor (Tans et al. [5]), a ballistic palladium-contacted transistor (Javey et al. [11]), a 16-bit RISC-V microprocessor with more than 14,000 transistors (Hills et al. [6]) and a tensor processing unit with 3,000 transistors (Si et al. [7]). Dotted lines mark the report of multi-walled tubes (Iijima [1]) and the first nanotube computer (Shulaker et al. [14]), whose transistor count is not plotted. (b) Ranges of tensile strength (11 to 63 GPa) and Young's modulus (270 to 950 GPa) measured on the outer shells of 19 multi-walled tubes by Yu et al. [8].

Panel (a) of Figure 4 is not a scaling law. The two systems at the right were built for different goals; the later one simply has fewer transistors. It shows the time scale: each step from device to circuit to system took the better part of a decade, and each needed progress in materials (purity, alignment, contacts) more than in single-tube physics. Panel (b) belongs to mechanics, and we return to it with composites.

5.2 Interconnects and transparent conductors

Metallic tubes are attractive as wires because they tolerate very high current densities. The multi-walled tubes of Frank and co-workers already carried stable densities above 10^7 A cm^{-2} while conducting ballistically, without dissipating heat along their length [13]. Integrating such wires at fine pitch, with good contacts, is the unsolved part.

Thin random networks of tubes also make transparent electrodes. Light passes through the open space between tubes while current percolates along the connected network, so a film only a few tubes thick can conduct and still let most light through. Such films are studied as flexible alternatives to oxide electrodes.

5.3 Sensors

In a single-walled tube every atom sits on the surface, so adsorbed molecules that donate or withdraw charge change its resistance. A gas such as NO_2, which pulls electrons away, and one such as NH_3, which gives them up, push the resistance of a semiconducting tube in opposite directions, and the response can be read at room temperature. The same principle now underlies biological sensing. A 2025 review of

transistor biosensors built on nanotubes describes devices for cancer biomarkers, infectious disease antigens and markers of neurodegeneration, often with floating-gate or microfluidic designs [12]. Its authors are frank about the gaps: scale-up, reproducibility between devices, and long-term stability are not yet solved.

5.4 Energy storage and composites

In batteries and supercapacitors nanotubes are used mostly as conductive additives and scaffolds. The physics is simple: a small mass of long conducting tubes can link many electrode particles into one network, because a long thin conductor reaches percolation at a far lower volume fraction than a round grain does. The practical difficulties are spreading the tubes evenly through an electrode and making them cheaply enough.

For composites the draw is mechanical. Yu and co-workers measured tensile strengths of 11 to 63 GPa and Young's moduli of 270 to 950 GPa for the outer shells of individual multi-walled tubes [8]. Yet these are single-tube values, and a composite only reaches them if load passes from the matrix into the tube and on to the inner shells; the sword-in-sheath failure is the warning.

5.5 Biomedical uses and toxicity

The clearest biomedical use so far is diagnostic, through the transistor biosensors above [12]. Anything that puts tubes inside the body faces a harder test, and shape is the problem. Injection studies in rodents have identified rigid multi-walled tubes as hazardous [15], and the comparison with asbestos fibres is hard to avoid. A 2025 review notes that the International Agency for Research on Cancer lists one material, MWCNT-7, as possibly carcinogenic to humans (Group 2B) and other multi-walled tubes as not classifiable; it also argues that two-year animal studies show both thick rigid and thin flexible tubes to be carcinogenic in test animals, and that the classification should be revisited [15]. Any biomedical use therefore has to control length, rigidity and clearance from the start.

6. Challenges and Outlook

Purity comes first. The tensor processor used semiconducting purity of 99.9999 percent [7]. At that level a chip with a billion tube segments would still contain about a thousand metallic ones, so circuit design has to tolerate them, as Shulaker and Hills did [14], [6]. Growth at a single chirality would remove the problem at its source, but it is not yet reliable enough to depend on.

Placement is next. Tubes must land aligned, at uniform pitch and density, across a 300 mm wafer, the size industrial lines use. Contacts are the third problem. Palladium removed the barrier for holes in single devices [11]; making low-resistance contacts reproducible across a wafer, for electrons as well as holes, is another matter.

Variability ties these together. Every tube has its own diameter, so its own gap, and its own defects [6]. Cost matters too: every sorting step adds expense, and scale-up remains a stated barrier in sensing [12].

Safety runs across all of it. The evidence on rigid multi-walled tubes [15] means exposure during production and disposal has to be designed out from the start.

Will nanotube logic reach commercial fabrication? The physics does not stand in the way. The open problems are in materials and manufacturing.

7. Conclusion

A reader who has come this far can take one tube, write down its chiral index, and predict its diameter, whether it conducts, roughly what gap it has, and where its breathing mode should appear in a Raman spectrum. That chain of reasoning, from a pair of integers to a measurable number, is the reason nanotubes became a model system for low-dimensional physics. It has held up under scanning tunnelling microscopy, optical spectroscopy and transport measurements, apart from the curvature gaps and excitonic shifts that refine it. The main open question is not about the physics of a single tube. It is whether billions of tubes can be grown or sorted, placed and contacted with the uniformity that a commercial process requires.

References

[1] S. Iijima, "Helical microtubules of graphitic carbon," Nature, vol. 354, no. 6348, pp. 56-58, Nov. 1991, doi: 10.1038/354056a0.

[2] R. Saito, M. Fujita, G. Dresselhaus, and M. S. Dresselhaus, "Electronic structure of chiral graphene tubules," Appl. Phys. Lett., vol. 60, no. 18, pp. 2204-2206, May 1992, doi: 10.1063/1.107080.

[3] N. Hamada, S. Sawada, and A. Oshiyama, "New one-dimensional conductors: Graphitic microtubules," Phys. Rev. Lett., vol. 68, no. 10, pp. 1579-1581, Mar. 1992, doi: 10.1103/PhysRevLett.68.1579.

[4] J. W. G. Wildöer, L. C. Venema, A. G. Rinzler, R. E. Smalley, and C. Dekker, "Electronic structure of atomically resolved carbon nanotubes," Nature, vol. 391, no. 6662, pp. 59-62, Jan. 1998, doi: 10.1038/34139.

[5] S. J. Tans, A. R. M. Verschueren, and C. Dekker, "Room-temperature transistor based on a single carbon nanotube," Nature, vol. 393, no. 6680, pp. 49-52, May 1998, doi: 10.1038/29954.

[6] G. Hills, C. Lau, A. Wright, S. Fuller, M. D. Bishop, T. Srimani, P. Kanhaiya, R. Ho, A. Amer, Y. Stein, D. Murphy, Arvind, A. Chandrakasan, and M. M. Shulaker, "Modern microprocessor built from complementary carbon nanotube transistors," Nature, vol. 572, no. 7771, pp. 595-602, Aug. 2019, doi: 10.1038/s41586-019-1493-8.

[7] J. Si, P. Zhang, C. Zhao, D. Lin, L. Xu, H. Xu, L. Liu, J. Jiang, L.-M. Peng, and Z. Zhang, "A carbon-nanotube-based tensor processing unit," Nat. Electron., vol. 7, no. 8, pp. 684-693, Jul. 2024, doi: 10.1038/s41928-024-01211-2.

[8] M.-F. Yu, O. Lourie, M. J. Dyer, K. Moloni, T. F. Kelly, and R. S. Ruoff, "Strength and breaking mechanism of multiwalled carbon nanotubes under tensile load," Science, vol. 287, no. 5453, pp. 637-640, Jan. 2000, doi: 10.1126/science.287.5453.637.

[9] A. Jorio, R. Saito, J. H. Hafner, C. M. Lieber, M. Hunter, T. McClure, G. Dresselhaus, and M. S. Dresselhaus, "Structural (n, m) determination of isolated single-wall carbon nanotubes by resonant Raman scattering," Phys. Rev. Lett., vol. 86, no. 6, pp. 1118-1121, Feb. 2001, doi: 10.1103/PhysRevLett.86.1118.

[10] H. Telg, J. Maultzsch, S. Reich, F. Hennrich, and C. Thomsen, "Chirality distribution and transition energies of carbon nanotubes," Phys. Rev. Lett., vol. 93, no. 17, Art. no. 177401, Oct. 2004, doi: 10.1103/PhysRevLett.93.177401.

[11] A. Javey, J. Guo, Q. Wang, M. Lundstrom, and H. Dai, "Ballistic carbon nanotube field-effect transistors," Nature, vol. 424, no. 6949, pp. 654-657, Aug. 2003, doi: 10.1038/nature01797.

[12] J. Sengupta and C. M. Hussain, "Carbon nanotube-based field-effect transistor biosensors for biomedical applications: Decadal developments and advancements (2016-2025)," Biosensors, vol. 15, no. 5, Art. no. 296, May 2025, doi: 10.3390/bios15050296.

[13] S. Frank, P. Poncharal, Z. L. Wang, and W. A. de Heer, "Carbon nanotube quantum resistors," Science, vol. 280, no. 5370, pp. 1744-1746, Jun. 1998, doi: 10.1126/science.280.5370.1744.

[14] M. M. Shulaker, G. Hills, N. Patil, H. Wei, H.-Y. Chen, H.-S. P. Wong, and S. Mitra, "Carbon nanotube computer," Nature, vol. 501, no. 7468, pp. 526-530, Sep. 2013, doi: 10.1038/nature12502.

[15] O. H. M. Ahmed, A. Naiki-Ito, S. Takahashi, W. T. Alexander, D. B. Alexander, and H. Tsuda, "A review of the carcinogenic potential of thick rigid and thin flexible multi-walled carbon nanotubes in the lung," Nanomaterials, vol. 15, no. 3, Art. no. 168, Jan. 2025, doi: 10.3390/nano15030168.